

## Effect of Entrance Channel Parameters on Incomplete Fusion Reactions

**A. Agarwal<sup>1</sup>, M. Kumar<sup>1</sup>, S. Prajapati<sup>1</sup>, S. Dutt<sup>2</sup>, I.A. Rizvi<sup>2</sup>,  
R. Kumar<sup>3</sup>, A.K. Chaubey<sup>4</sup>**

<sup>1</sup>Department of Physics, Bareilly College, Bareilly 243 005 India

<sup>2</sup>Department of Physics, Aligarh Muslim University, Aligarh 202 002 India

<sup>3</sup>NP Group, Inter University Accelerator Centre, New Delhi 110 067 India

<sup>4</sup>Department of Physics, A. A. University, Addis Ababa, Ethiopia

**Abstract.** An attempt has been made to have exclusive information on effect of various entrance channel parameters on the onset of incomplete fusion in heavy ion induced reactions at energies at 4 - 7 MeV/A. A number of experiments have been performed by our group to measure the excitation function and forward recoil range distribution of various evaporation residues populated via complete fusion and/or incomplete fusion of  $^{16}\text{O}$  with different targets. The experimental excitation functions have been analysed in the frame work of compound nucleus decay using statistical model code PACE-4. Analysis of data suggests the existence of incomplete fusion even at energies as low as near barrier energies where complete fusion is supposed to be the sole contributor. Further more, in order to understand incomplete fusion reactions in a more conclusive way, the incomplete fusion fraction has been analyzed with the existing data for  $\alpha$ - cluster projectiles with different targets of low, medium and heavy mass region. The study of percentage incomplete fusion fraction for different projectile target combinations deduced from experimentally measured excitation functions of individual reaction product shows strong dependence on projectile energy, mass asymmetry of interacting partners and  $\alpha - Q$  value of the projectile.

### 1 Introduction

The study of incomplete fusion (ICF) reaction dynamics, at energies in the vicinity of coulomb barrier(CB) has been a topic of extensive discussion among experimental as well as theoretical nuclear physicists in the recent past couple of years. [1–6] This debate has been continuously innovated with the observation of ICF near coulomb barrier, where complete fusion(CF) is expected to be the sole contributor to the total reaction cross-section [2, 6]. In the case of CF an equilibrated compound nucleus (CN) is formed involving all nucleonic degrees of freedom of the interacting partners which decay by evaporating low energy nucleons and alpha particles. It involves full momentum transfer of the projectile to the target. However ICF has been found to be competing fusion like processes [7, 8] forming a reduced excited composite system with relatively lower

mass and excitation energy compared to the completely fused composite system, due to prompt emission of  $\alpha$  - clusters in the forward cone with almost same velocity as that of incident ion beam at the initial stage of interaction. Here only a fraction of momentum essentially equal to mass of the projectile that fused is transferred. Britt and Quinton [9] were the first who observed ICF reactions at relatively higher energies  $\approx 10.5$  MeV/A. Particle -  $\gamma$  coincidence measurements by Inamura *et al* [10] has also contributed a great deal to the understanding of ICF dynamics. The important signatures of ICF are (i) higher production yield (cross-section) for a particular radioisotope (essentially through ICF) than those predicted by fusion evaporation model [11]. (ii) The forward recoil range distribution (FRRD) of heavy residues shows relatively low range of components suggesting incomplete momentum transfer [12]. (iii) The outgoing fast alpha particles have forward peaked angular distribution and energy spectrum peaked at beam velocity [9] (iv) The spin distribution of evaporation residues populated by ICF are found to be distinctly different from those of CF [7].

Since the observation of ICF reaction dynamics, a number of theoretical models have been proposed to explain the mechanism of ICF reaction, such as break-up fusion model [13] sum rule model [14], promptly emitted particle model [15], multistep direct reaction model [16] hot spot model [17] and exciton model [18]. All these models have been used to explain the experimental data obtained using projectile energies above 10 MeV/A or so. However Teserruya *et al* found evidences of ICF from time of flight measurements of evaporation residues at 5.5 MeV/A [19] and Parker *et al* observed forward peaked alpha particles due to ICF in the reaction of 6 MeV/A low  $z$  heavy ions on  $^{51}\text{V}$  [20]. Though a lot of work with variety of studies exist in literature [1, 2, 6, 7, 12, 21], the dynamics of ICF at low incident energies is still not fairly well understood. The most debated issues related to ICF in present scenario includes probing the effect of various entrance channel parameters on ICF reactions such as projectile structure, projectile energy, entrance channel mass asymmetry, angular momentum involved,  $\alpha - Q$  value and/or binding energy of the projectile. Hence in order to explore the low energy incomplete fusion and have a consistent systematic, our group has under taken a program to study low energy ICF reactions and performed a number of experiments using national accelerator facility and the findings have been/will be appeared in our recent publications [6, 12, 22, 23]. In this paper an attempt has been made to summarize our recent findings and develop a systematic for low energy ICF reactions.

## 2 Experimental Details and Data Reduction Procedure

The experiments have been carried out using  $^{16}\text{O}$  and  $^{12}\text{C}$  beams at Inter University Accelerator Centre (IUAC), New Delhi, India. Targets of different spectroscopically pure materials of thickness  $1.1 \text{ mg/cm}^2$  -  $1.5 \text{ mg/cm}^2$  were prepared either by vacuum evaporation or rolling technique. The thickness of each target and aluminum catcher foil was separately measured through weighing and

### Effect of Entrance Channel Parameters on Incomplete Fusion Reactions

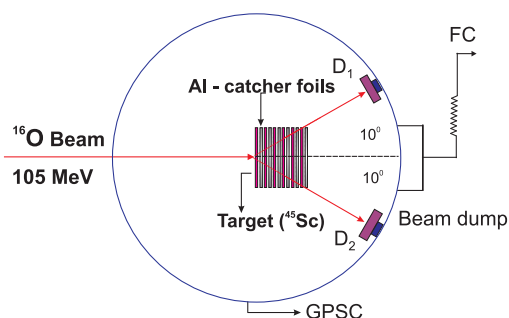


Figure 1. Typical stacked foil arrangement used for excitation function measurements.

by  $\alpha$  - transmission method respectively. The well established activation technique followed by off line  $\gamma$ -ray spectroscopy was used for the present measurements. For measurement of excitation functions of individual reaction product populated via CF and/or ICF, stacks of target foils each backed by Al-foils of suitable thickness required to stop the most energetic recoiling residue were irradiated independently by  $^{16}\text{O}$  and  $^{12}\text{C}$  beams of energy range 4 - 6 MeV/A in general purpose scattering chamber (GPSC). The chamber has a facility of invacuum transfer of targets, which minimizes the time lapse between the stopping of irradiation and beginning of counting. A typical stacked foil arrangement used for excitation function measurements is shown in Figure 1. The incident flux of projectile beam was determined from the charge collected in the Farady cup as well as from the counts of the two Rutherford monitors kept at  $\pm 10^0$  to the beam direction. The two sets of values were found to agree with each other, any discrepancy between them being within the 5% of the values. Keeping in mind the half lives of the residues of interest, the stacks were irradiated for 8 - 12 hrs. Pre-calibrated HPGe detector coupled to a CAMAC based data acquisition system CANDLE [24] has been used to record the induced activity in the target-catcher assembly.

The average time between the end of the irradiation and the beginning of the measurements with HPGe was  $\approx 15$  min. The nuclear spectroscopic data used in the evaluation and measurement of cross sections were taken from the radioactive isotopes data table of Browne and Firestone [25] The spectrometer was calibrated for energy, and efficiency using various standard sources, i.e.  $^{152}\text{Eu}$ ,  $^{60}\text{Co}$ ,  $^{57}\text{Co}$ , and  $^{133}\text{Ba}$ . Details of geometry-dependent efficiency measurements used in this work are similar to those used by Agarwal *et al* [11]. Figure 2 shows a typical  $\gamma$  - ray spectrum obtained at 81.15 Mev in the interaction of  $^{16}\text{O}$  and  $^{55}\text{Mn}$ . The residues produced from various reaction channels were identified by their characteristic  $\gamma$  - ray and decay curve analysis. The details of the experimental arrangements, formulations, and data reduction procedures used in the present work are similar to those in the work of Agarwal *et al* [11].

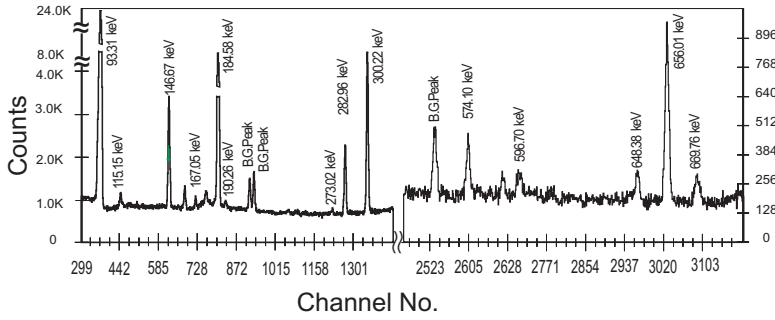


Figure 2. Typical  $\gamma$ -ray spectrum of  $^{16}\text{O} + ^{55}\text{Mn}$  system at 81.15 MeV projectile energy. The energies of the identified peaks are also given in keV.

The standard formulation reported in Ref. [11, 12] was used to determine the production cross sections of various reaction products. The various factors that may introduce errors and uncertainties in the present cross-section measurements and their estimates are the following:

(i) The nonuniform thickness of samples may lead to uncertainty in determining the number of target nuclei. To check the extent of the nonuniformity of the sample, the thickness of each sample was measured at different positions using  $\alpha$ -transmission method. It is estimated that the error in the thickness of the sample materials is less than 1%. (ii) Fluctuation in the beam current may result in variation of the incident flux; proper care was taken to keep the beam current constant as much as possible. The error due to this factor was incorporated by taking the weighted average of the beam current and is estimated to be less than 2%. (iii) The dead time in the spectrometer may lead to a loss in the counts. By suitably adjusting the sample-detector distance, the dead time was kept below 10%. These errors exclude uncertainty of the nuclear data, such as branching ratio, decay constant, etc., which have been taken from Ref. [25]. (iv) Uncertainty in determining the geometry-dependent detector efficiency may also introduce some error, which is estimated to be less than 2%. (v) Errors due to a decrease in the oxygen ion beam intensity caused by scattering while transferring through the stack are estimated to be less than 1%. Attempts were made to minimize the uncertainties caused by all the above factors. The overall error in the present work is estimated to be less than or equal to 17%.

### 3 Interpretation of Excitation Functions: First Hint to ICF Dynamics

The first hint of ICF dynamics in heavy ion induced reactions may be obtained by comparing the experimentally measured EFs with the theoretical predictions obtained using statistical model based computer codes PACE-4 [26] and ALICE-91 [27]. It has been observed that for low  $Z$  targets the Alice-91 works well while

Effect of Entrance Channel Parameters on Incomplete Fusion Reactions

for targets of higher mass region PACE-4 predictions are found to be in good agreement for complete fusion channels. It has now well observed/established that the enhancement of measured production cross-sections for evaporation residues populated through  $\alpha$  emitting production channels over theoretically calculated values is mainly due to the presence of ICF along with CF dynamics in heavy ion interactions above barrier energies [11]. As a representative case the comparison of total experimentally measured cross-section of all  $xn/pxn$  channels i.e.

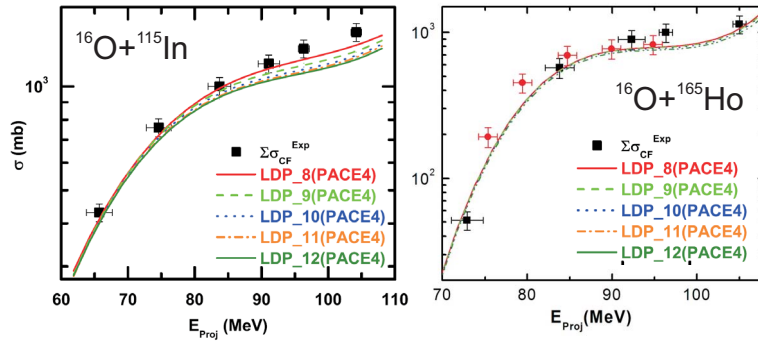


Figure 3. Sum of measured EFs for all CF channels along with PACE 4 calculations for  $^{16}\text{O} + ^{165}\text{Ho}$  and  $^{16}\text{O} + ^{115}\text{In}$  systems.

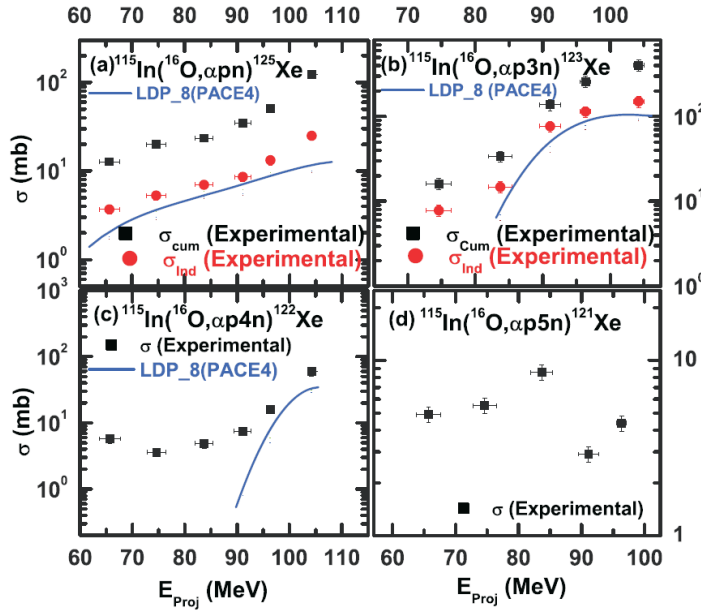


Figure 4. Experimentally measured EFs of all  $(\alpha pxn)(x = 1, 3 - 5)$  channels.

$[\Sigma\sigma_{cf}^{expt}]$  with PACE-4 predictions i.e.  $[\Sigma\sigma_{cf}^{theo}]$  for  $^{16}\text{O} + ^{115}\text{In}$  and  $^{16}\text{O} + ^{165}\text{Ho}$  are shown in Figure 3. The experimentally measured EFs for  $\alpha$ -emitting channels such as  $\alpha pxn$  channels are also shown in Figure 4. Due to the involvement of  $\alpha$ -particle emission, both CF and ICF are considered to be responsible for reaction modes, namely, (i) by CF of  $^{16}\text{O}$  followed by the formation of an excited compound nucleus, from which evaporation of neutrons, protons, and  $\alpha$ -particles may take place, or (ii) first  $^{16}\text{O}$  breaks into  $\alpha$  clusters in the nuclear field of target such as  $(\alpha + ^{12}\text{C})$  or  $(^8\text{Be} + ^8\text{Be})$  and then one of the fragments fuses with the target and the other fragment goes into the forward direction elastically. In this case the excited composite system is less in mass and charge than that in case of CF and hence is here referred to as ICF. Therefore, the reaction mechanism for the population of all observed  $\alpha$ -emitting channels in this case is expected to be CF and/or ICF. From the EFs of all the  $\alpha pxn$  channels, we can see enhancement over the theoretical predictions of PACE-4. Since the statistical model code PACE-4 does not take into account ICF processes, the observed enhancement in the experimentally measured EFs points toward the contribution of ICF in the production of these residues. Hence, an attempt has been made to study the ICF probability. The ICF contribution in the production of all  $\alpha$ -emitting channels has been deduced as;  $\Sigma\sigma_{ICF} = \Sigma\sigma_{expt} - \Sigma\sigma_{PACE-4}$ . In order to see how does ICF contributes to the total fusion cross section ( $\sigma_{TF} = \Sigma\sigma_{CF} + \Sigma\sigma_{ICF}$ ), the sum of CF cross sections of all channels ( $\Sigma\sigma_{CF}$ ) and  $\sigma_{TF}$  as a function of incident projectile energy are plotted in Figure 5. Different solid lines are drawn to guide the eyes. The increasing separation between  $\Sigma\sigma_{CF}$  and  $\sigma_{TF}$  indicates the energy dependence of projectile breakup and strong dependency of ICF fraction on incident projectile energy. For better visualization of increasing ICF contribution with projectile energy, the value of  $\Sigma\sigma_{ICF}$  is plotted in the inset of Figure 5.

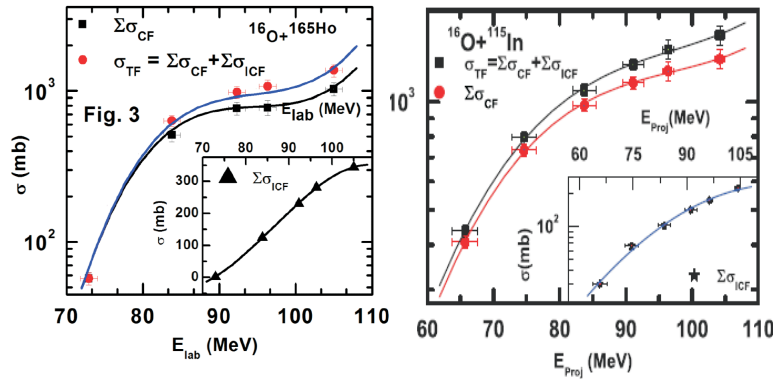


Figure 5. The Total fusion cross section ( $\sigma_{TF}$ ) and sum of the CF cross section ( $\Sigma\sigma_{CF}$ ) of all channels. In the inset, the sum of all the ICF cross-section ( $\Sigma\sigma_{ICF}$ ) as a function of projectile energy as shown.

## 4 Entrance Channel Dependence of ICF

### 4.1 Projectile energy and mass assymetry dependance of ICF

To study the dependence of ICF on various entrance channel parameters the percentage ICF fraction ( $F_{ICF}$ ) is evaluated using the relation

$$F_{ICF}(\%) = \frac{\Sigma\sigma_{ICF}}{\sigma_{TF}} X 100 \quad (1)$$

where  $\Sigma\sigma_{ICF}$  is the sum of incomplete fusion cross sections and  $\sigma_{TF}$  is total fusion cross section, respectively, at the considered energies. The value of  $F_{ICF}$  obtained from the excitation function measurements of  $^{16}\text{O} + ^{115}\text{In}$  [22] and  $^{16}\text{O} + ^{165}\text{Ho}$  [23] systems, as a function of normalized projectile energy ( $E_{Proj}/V_{CB}$ ), is plotted in Figure 6. As can be seen from this figure, the  $F_{ICF}$  increases with the projectile energy. Moreover, it can also percentage ICF contribution for the system  $^{16}\text{O} + ^{165}\text{Ho}$  increases more rapidly than that of the system  $^{16}\text{O} + ^{115}\text{In}$  [30], which can be understood in terms of mass-asymmetry systematics of interacting partners, established by Morgenstern et al. [28]. According to the mass-asymmetry systematics, the ICF probability should be more for more a mass-asymmetric system than for a mass symmetric system. The mass asymmetry of any system can be denoted as  $M_a = A_T/(A_T + A_P)$ , where  $A_T$  and  $A_P$  are the masses of the target and of the projectile, respectively. Hence, the calculated mass-asymmetries of the systems  $^{16}\text{O} + ^{165}\text{Ho}$  and  $^{16}\text{O} + ^{115}\text{In}$  are 0.911 and 0.877, respectively. Therefore, Figure 6 reflects that these two systems follow the mass-asymmetry systematic even at low incident energies, while Morgenstern et al. [28] observed this systematics at relatively higher energies  $\approx$

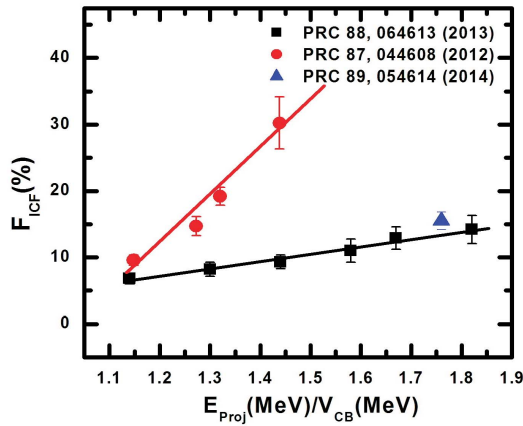


Figure 6. The incomplete fusion fraction  $F_{ICF}$  as function of normalized projectile energy. The red circles are for  $^{16}\text{O} + ^{165}\text{Ho}$  system while black squares and blue triangle are for  $^{16}\text{O} + ^{115}\text{In}$  system.

10 to 25 MeV/nucleon. Moreover, this rapid increase in Figure 6 can also be explained by the systematics introduced by Gomes et al. [29, 30], which shows dependence of ICF on Coloumb repulsion ( $Z_P.Z_T$ ) of the interacting partners. Hence, the larger Coloumb repulsion in the  $^{16}\text{O} + ^{165}\text{Ho}$  than in the  $^{16}\text{O} + ^{115}\text{In}$  system leads to a higher probability for ICF. Also, it was observed by Inamura et al. [10] that ICF processes are mainly due to the peripheral interactions. This situation may also be one of the reasons for the rapid increase, due to the larger angular momenta associated with the system  $^{16}\text{O} + ^{165}\text{Ho}$  than that associated with the system  $^{16}\text{O} + ^{115}\text{In}$ .

#### 4.2 Projectile structure dependance of ICF

To have exclusive/concluding information on the effect of mass-asymmetry systematics the ICF fraction for our systems along with those available in literature for  $^{12}\text{C}$ ,  $^{16}\text{O}$  and  $^{20}\text{Ne}$  projectiles at constant  $v_{rel} = 0.0566c$  are plotted in Figure 7. The data points for 12 different projectile target combinations clearly suggest more ICF probability for more mass-asymmetric system. Further it can also be seen that for  $^{20}\text{Ne}$  induced reactions the ICF fraction possess the highest value while for  $^{12}\text{C}$  induced reactions ICF fraction is found to be least among  $^{12}\text{C}$ ,  $^{16}\text{O}$  and  $^{20}\text{Ne}$  projectiles. This clearly shows that projectile structure effect also accounts for ICF reactions.

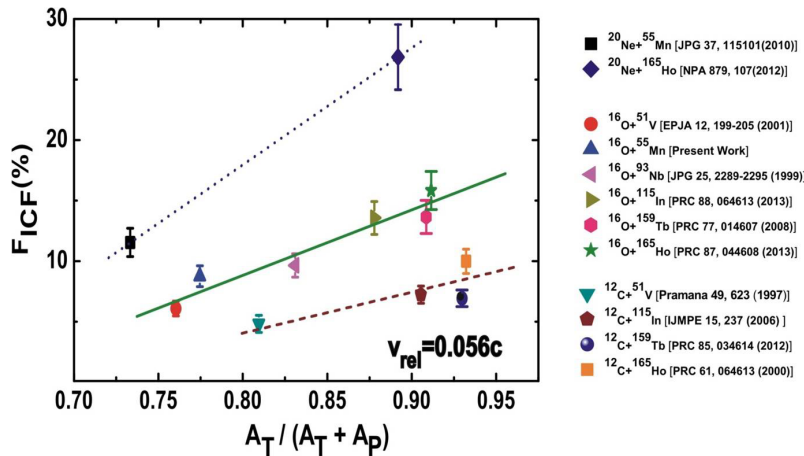


Figure 7. The incomplete fusion fraction  $F_{ICF}$  as function of mass asymmetry at  $v_{rel} = 0.056c$  for different projectile target systems

#### 4.3 $\alpha$ -Q value dependance of ICF

The onset of projectile structure dependence of ICF can be explored by the study of projectile structure dependance of ICF reactions in the nuclear field of targets of different mass ranges. The break-up of different projectiles in the nuclear



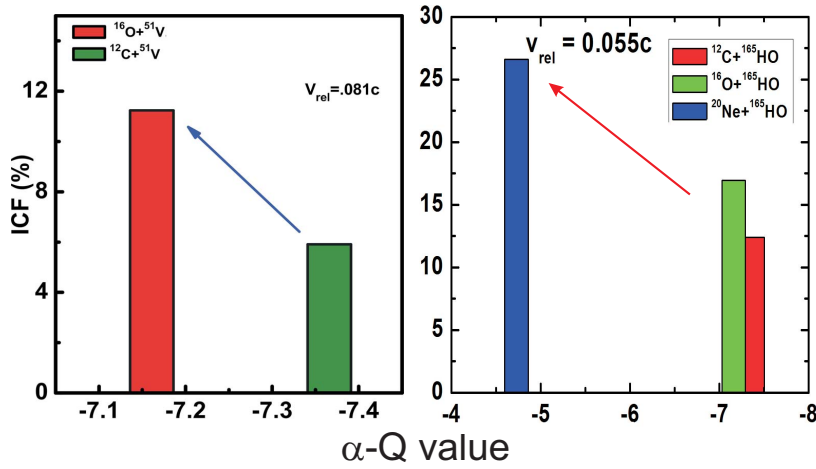


Figure 8. The incomplete fusion fraction  $F_{ICF}$  as function of  $\alpha$  Q-value for the systems  $^{12}\text{C} + ^{165}\text{Ho}$ ,  $^{16}\text{O} + ^{165}\text{Ho}$ ,  $^{20}\text{Ne} + ^{165}\text{Ho}$ ,  $^{12}\text{C} + ^{51}\text{V}$  and  $^{16}\text{O} + ^{51}\text{V}$ .

field of same target can be understood in terms of  $\alpha$ -Q value of the projectile. In Figure 8 the  $F_{ICF}$  for same target using three different projectiles with targets of different mass region are shown as a function of  $\alpha$ -Q value of projectiles. The  $\alpha$ -Q values for  $^{12}\text{C}$ ,  $^{16}\text{O}$  and  $^{20}\text{Ne}$  are -7.37 MeV, -7.16 MeV and -4.73 MeV respectively, making  $^{20}\text{Ne}$  more unstable for the breakup in the nuclear field of the same target. It is evident in Figure 8 that the probability of ICF is found to be less for larger negative  $\alpha$ -Q value projectile. Hence from the data presented in the figure, it can be inferred that for a particular  $v_{rel}$  the ICF is strongly governed by the kind of projectile and  $\alpha$ -Q value is an important entrance channel parameter which essentially dictates the probability of ICF.

## 5 Conclusion

In this paper recent results on observation of low energy incomplete fusion are presented. The observed enhancement in experimentally measured excitation functions may be assumed to come from prompt breakup of projectile into  $\alpha$ -cluster leading to incomplete fusion process. The ICF fraction has been deduced from the analysis of Excitation functions in the framework of statistical model code PACE-4. A systematic study of the ICF fraction has been presented as a function of various entrance channel parameters. The percentage fraction of ICF is found to increase with projectile energy and mass asymmetry for individual projectiles. The effect of  $\alpha$  Q-value on ICF reactions has been observed for strongly bound  $\alpha$  structure projectiles. The ICF fraction has been observed to decrease for large negative  $\alpha$ -Q value projectiles. Hence the  $\alpha$ -Q value may be assigned to be responsible for the projectile structure effect. Many other en-

trance channel parameters may affect ICF reactions, and hence more systematic studies are required using different alpha and non alpha structure projectiles.

### Acknowledgements

The authors are thankful to the Director IUAC, New Delhi for providing all the necessary facilities to carry out the experiments. Thanks are also due to the Principal, Bareilly College, Bareilly for his keen interest in the present study. Financial support from IUAC through UFR research project to one of author (Avinash Agarwal) is also highly acknowledged.

### References

- [1] V.R. Sharma et al., *Nucl. Phys. A* **964** (2016) 182.
- [2] R. Ali et al., *J. Phys G: Nucl. Part. Phys.* **37** (2010) 115101.
- [3] P.R.S. Gomes et al., *Phys. Rev. C* **84** (2011) 014615.
- [4] D.J. Hinde and M. Dasgupta *Phys. Rev. C* **81** (2010) 064611 and references therein.
- [5] A. Diaz-Torres *J. Phys. G: Nucl. Part. Phys.* **37** (2010) 075109.
- [6] A. Agarwal et al., *Japanese Physical Society (JPS) Conference Series* [Online journal] **Vol 6** (2015) 030095.
- [7] P.P. Singh et al., *Phys. Rev. C* **80** (2009) 064603.
- [8] D. Singh et al., *Phys. Rev. C* **83** (2011) 054604.
- [9] H.C. Britt and A.R. Quinton, *Phys. Rev. C* **124** (1961) 877.
- [10] T. Inamura et al., *Phys. Lett. B* **68** (1977) 51.
- [11] A. Agarwal et al., *Int. J. Mod. Phys. E* **17** (2008) 1393.
- [12] K. Kumar et al., *Phys. Rev. C* **89** (2014) 054614.
- [13] T. Udagawa and T. Tamura, *Phys. Rev. Lett* **45** (1980) 1311.
- [14] J. Wilczynski et al., *Nucl. Phys. A* **373** (1982) 109.
- [15] J.P. Bondroff et al., *Nucl. Phys. A* **333** (1980) 285.
- [16] V.I. Zagebaev, *Ann. Phys. NY* **197** (1990) 33.
- [17] R. Weiner and M. Westrom, *Nucl. Phys. A* **386** (1977) 282.
- [18] M. Blann, *Phys. Rev. C* **24** (1981) 89.
- [19] I. Tserruya et al., *Phys. Rev. Lett.* **60** (1988) 14.
- [20] D.J. Parker, J.J. Hoga and J. Asher, *Phys. Rev. C* **35** (1987) 35.
- [21] P.P. Singh et al., *Phys. Lett. B* **671** (2009) 20.
- [22] K. Kumar, et al., *Phys. Rev. C* **88** (2013) 064613.
- [23] K. Kumar, et al., *Phys. Rev. C* **87** (2013) 044608.
- [24] B.P. Ajith Kumar et al., *CANDLE Collection and Analysis of Nuclear Data using Linux Network DAE SNP Kolkata*(2001).
- [25] E. Browne and R.B. Firestone, *Table of Radioactive Isotopes* (Wiley, New York, 1986).
- [26] A. Gavron, *Phys. Rev. C* **21** (1980) 230.
- [27] M. Blann, *NEA Data Bank Gif-Sur-Yvette, France Report PSR - 146*.
- [28] H. Morgenstern et al., *Phys. Rev. Lett.* **52** (1984) 1104.
- [29] P.R.S. Gomes et al., *Phys. Rev. C* **73** (2006) 064606.
- [30] P.R.S. Gomes et al., *Phys. Lett. B* **601** (2004) 20.